Biochemical and Biophysical Research Communications 427 (2012) 5–10

Contents lists available at SciVerse ScienceDirect

Biochemical and Biophysical Research Communications

journal homepage: www.elsevier.com/locate/ybbrc

Characterization of p75$^+$ ectomesenchymal stem cells from rat embryonic facial process tissue

Xiujie Wen, Luchuan Liu, Manjing Deng, Li Zhang, Rui Liu, Yongjun Xing, Xia Zhou, Xin Nie *

Department of Stomatology, Daping Hospital & Research Institute of Surgery, Third Military Medical University, Chongqing 400042, China

ARTICLE INFO

Article history:
Received 9 August 2012
Available online 12 September 2012

Keywords:
Ectomesenchymal cells
p75 neurotrophin receptor
Embryonic facial process

ABSTRACT

Several populations of stem cells, including those from the dental pulp and periodontal ligament, have been isolated from different parts of the tooth and periodontium. The characteristics of such stem cells have been reported as well. However, as a common progenitor of these cells, ectomesenchymal stem cells (EMSCs), derived from the cranial neural crest have yet to be fully characterized. The aim of this study was to better understand the characteristics of EMSCs isolated from rat embryonic facial processes. Immunohistochemical staining showed that EMSCs had migrated to rat facial processes at E11.5, while the absence of epithelial invagination or tooth-like epithelium suggested that any epithelial–mesenchymal interactions were limited at this stage. The p75 neurotrophin receptor (p75NTR), a typical neural crest marker, was used to select p75NTR-positive EMSCs (p75$^+$ EMSCs), which were found to show a homogeneous fibroblast-like morphology and little change in the growth curve, proliferation capacity, and cell phenotype during cell passage. They also displayed the capacity to differentiate into diverse cell types under chemically defined conditions *in vitro*. p75$^+$ EMSCs proved to be homogeneous, stable *in vitro* and potentially capable of multiple lineages, suggesting their potential for application in dental or orofacial tissue engineering.

1. Introduction

There has been significant recent progress in the field of dental tissue regeneration, which can be attributed to major advances in our understanding of dental stem cells such as those from the dental pulp and periodontal ligament [1–3]. However, it has been proposed that such cells isolated from mature tooth tissues are progenitor cells already committed to certain dental cell lineages and not multipotent mesenchymal stem cell populations [4]. Tooth development research has indicated that ectomesenchymal stem cells (EMSCs) derived from the cranial neural crest may be a common progenitor of dental mesenchymal stem cells, including dental papilla and dental follicle cells [5]. During tooth morphogenesis, odontogenic genes in EMSCs are triggered by the epithelial–mesenchymal interaction, whereby EMSCs finally give rise to the cells of the dental papilla and dental follicle, subsequently forming dentin, pulp, cementum and periodontal ligaments [6,7]. Therefore, the characterization of EMSCs derived from the cranial neural crest is important for assessing opportunities for periodontal/dental regeneration and tissue-engineering approaches in the repair of orofacial structures and understanding normal and abnormal orofacial development.

Our previous studies have demonstrated the isolation, *in vitro* multipotency and peripheral nerve regenerative capacity of EMSCs from the first branchial arch [8,9]. These cells, isolated using the enzymatic dissociation method, are marked by morphologic heterogeneity and tendency to spontaneously differentiate along smooth muscle or osteoblast lineages. However, their characterization does pose challenges.

p75 neurotrophin receptor (p75NTR), which is abundantly expressed in neuronal precursor cells, is considered a typical neural crest marker [10,11] and has previously been used to isolate neural crest-derived stem cells from embryonic mandibular processes using magnetic-activated cell sorting (MACS) prior to investigation of their multi-potentiality [12]. The aim of this study was to purify EMSCs via fluorescence activated cell sorting (FACS) using p75NTR and to characterize the *in vitro* proliferative capacity, cell phenotype and multipotential differentiation of p75NTR-positive EMSCs (p75$^+$ EMSCs), thereby providing an EMSC model for studies of tooth development and regeneration.

2. Materials and methods

2.1. Experimental animals

Sprague–Dawley (SD) rats that were 11.5 days into embryonic development (E11.5) were provided by the Third Military Medical University Animal Laboratory. All procedures were approved by

* Corresponding author. Address: Department of Stomatology, Daping Hospital & Research Institute of Surgery, Third Military Medical University, 10, Daping Changjiang Branch Road, Yuzhong District, Chongqing 400042, China. Fax: +86 23 68715568.
E-mail address: dr.xinnie@gmail.com (X. Nie).

0006-291X/$ - see front matter © 2012 Elsevier Inc. All rights reserved.
http://dx.doi.org/10.1016/j.bbrc.2012.08.109

the Medical Ethics Committee of the Third Military Medical University.

2.2. Immunohistochemistry

The embryonic facial processes were dissected from the E11.5 SD rats and fixed in 4% paraformaldehyde. Hematoxylin and eosin (H.E.) staining and immunostaining were performed using the following primary antibodies: mouse anti-rat CD29, CD44, CD90, and CD105 (1:100, Santa Cruz, CA, USA); mouse anti-rat IgM Stro-1 (1:100, Abcam Inc., Cambridge, MA, USA); and rabbit anti-rat p75NTR (1:100, R&D Systems, Inc., Minneapolis, MN, USA). Sections were then incubated with secondary antibodies and stained with DAPI (4′,6-diamidino-2-phenylindole) (Sigma, USA), prior to observation with a confocal laser scanning microscope (TCS SP2; Leica Microsystems, Heidelberg, Germany).

2.3. Isolation and culture of EMSCs

Rat embryonic facial processes were harvested, minced into fine pieces, digested with 1% trypsin/l mM EDTA solution (Sigma, USA), filtered through a 75 μm mesh filter, centrifuged and cultured in Dulbecco's Modified Eagles Medium/Ham's F12 (DMEM/F12) (Gibco, USA) supplemented with 10% fetal bovine serum (FBS, Gibco, USA).

2.4. Sorting of $p75^+$ EMSCs

$p75^+$ EMSCs were selected using FACS as described previously [13]. Briefly, EMSCs at passage 3 were harvested and incubated in 1% BSA–PBS containing anti-p75NTR antibody for 30 min on ice prior to being incubated with anti-rabbit IgG-TRITC for another 30 min. $p75^+$ EMSCs were then collected using a FACS Calibur flow cytometer (BD Bioscience, San Jose, CA).

2.5. In vitro stability assays of $p75^+$ EMSCs

2.5.1. Proliferation activity

$p75^+$ EMSCs at passages 3 and 9 were seeded into 96-well plates at a density of 1×10^3 cells/well. The proliferative activities of these two cell populations were evaluated according to their growth curves, population doubling times, cell cycles and MTT assay results, as previously described [15].

2.5.2. Cell phenotype analysis

Flow cytometry was used to detect the expression of the following cell surface markers in $p75^+$ EMSCs at passages 3 and 9: CD29, CD44, CD90, CD105, Stro-1 and p75NTR, as previously described [16]. Briefly, approximately 5×10^5 cells were harvested and incubated overnight with primary antibodies according to the manufacturer's protocol before the addition of secondary antibodies. Cells were then analyzed with a FACS Calibur flow cytometer.

2.6. Multipotential differentiation assay of $p75^+$ EMSCs

2.6.1. Adipogenic differentiation

$p75^+$ EMSCs were seeded in 6-well plates at a density of 1×10^5 cells per well overnight and later incubated with adipogenic medium. After 10 days of culture, the cells were stained using Oil Red-O and observed with a digital inverted microscope (Leica, Cambridge, UK).

2.6.2. Osteogenic differentiation

After two weeks of culturing in osteogenic medium, $p75^+$ EMSCs were fixed and stained with Alizarin red. The mineralized nodules were then examined with a digital inverted microscope.

2.6.3. Chondrogenic differentiation

$p75^+$ EMSCs were seeded in 6-well plates and cultured in chondrogenic medium for two weeks. The differentiated cells were fixed and incubated in 1% (w/v) Alcian blue (Sigma, USA) for 30 min. Finally, 0.1 M HCl was used to remove any excess stain before the cells were observed with a digital inverted microscope.

2.6.4. Neuron-Like differentiation

The seeded $p75^+$ EMSCs were initially incubated with a pre-induction medium containing DMEM/F12 without FBS but containing 1 mM β-mercaptoethanol (Sigma, USA) and then incubated in a neurogenic medium as described previously [14]. After five days of culturing, the cells were fixed and incubated with an anti-neurofilament M (NF-M) (1:100, Santa Cruz, CA, USA) antibody, followed by secondary IgG-FITC (1:100) and DAPI. The cells subsequently were observed using a confocal laser scanning microscope.

2.6.5. RT-PCR assay

RT-PCR was performed as previously described [15] to further confirm the multipotential differentiation ability of the $p75^+$ EMSCs. The following primers were used, which are also detailed in Table 1: *lipoprotein lipase* (*LPL*) and *peroxisome*

Table 1
Specific primers used for RT-PCR.

Gene	Primer sequence	Product size (bp)	GenBank® accession no.
LPL	5′-GTATCGGGCCCAGCAACATTATCC-3′ 5′-GCCTTGCTGGGGTTTTCTTCATTC-3′	520	NM_012598
PPARγ	5′-AGGATCCATGAAGAACCTTTCATTTCTCCTA-3′ 5′-CCTTGCATCCCTCCAAAGCAT-3′	360	NM_013124
Col I	5′-CGTGACCAAAAACCAAAAGTGC-3′ 5′-GGGGTGGAGAAAGGAACAGAAA-3′	188	NM_Z78279
OCN	5′-ATGAGGACCCTCTCTCTGCTC-3′ 5′-CTAAACGGTGGTGCCATAGAT-3′	300	NM_340986
Col II	5′-GAAGCACATCTGGTTTGGAG -3′ 5′-TTGGGGTTGAGGGTTTTACA-3′	448	L48440
AGG	5′-TAGAGAAGAAGAGGGGTTAGG-3′ 5′-AGCAGTAGGAGCCAGGGTTAT-3′	322	J03485
NF-M	5′-GAAGGAAAAGAGGAGGAGGAG-3′ 5′-CAAGGACTGAGGAGGCACCC-3′	500	NM_017029
MAP-2	5′-TCGGCTCATTAACCAACCTC-3′ 5′-GAGCCACATTTGGAAGTCAC-3′	150	NM_013066
β-Actin	5′-CGGTTGGCCTTAGGGTTCAGGGGG-3′ 5′-CATCGTGGGCCGCTCTAGGCACCA-3′	248	NM_031144

proliferator-activated receptor-γ2 (*PPARγ2*) *mRNA* for adipogenesis, *osteocalcin* (*OCN*) and *type I collagen* (*Col I*) *mRNA* for osteogenesis, *Aggrecan* (*AGG*) and *collagen type II* (*Col II*) for chondrogenesis, and *microtubule-associated protein-2* (*MAP-2*) and *NF-M* for Neuron-Like Differentiation.

2.7. Statistical analysis

Data from the stability assays for the $p75^+$ EMSCs during cell passaging were statistically analyzed using the chi-square test and independent sample *t*-test (Student's unpaired *t*-test). The difference was considered to be statistically significant at $p < 0.05$.

3. Results

3.1. Immunohistochemistry of rat embryo facial processes

The dissected embryo facial processes are shown in Fig. 1A and B). H.E. staining (Fig. 1C–E) indicated that embryonic facial processes were composed of large numbers of mesenchymal cells with a thin covering layer of epithelium. There was no evidence of epithelial invagination or tooth-like epithelium, suggesting that epithelial–mesenchymal interactions might be limited at this stage. Immunofluorescence staining (Fig. 1F–L) demonstrated the positive expression of p75NTR, Stro-1, double p75NTR/Stro-1, CD29, CD44, CD90 and CD105, indicating that neural crest-derived EMSCs had migrated to and populated the rat embryonic facial processes at E11.5.

3.2. $p75^+$ EMSCs selection

In live cell sorting, $p75^+$ EMSCs accounted for 31.37% (Supplementary Fig. 1A and B) of the present cells. A morphologic investigation showed that EMSCs before selection were not homogeneous and that some cells were clustered in a mass (Supplementary Fig. 2A), whereas the selected $p75^+$ EMSCs displayed a homogeneous fibroblast-like morphology (Supplementary Fig. 2B).

3.3. In vitro stability of $p75^+$ EMSCs

The effects of nine passages on the growth, proliferation and cell phenotype of $p75^+$ EMSCs were investigated. Both the 3rd and 9th passages of $p75^+$ EMSCs began to grow exponentially at day 2, reaching a peak at days 8 and 9, respectively (Fig. 2A). The population doubling time (PDT) was calculated at 31.75 h for the 3rd passage $p75^+$ EMSCs and at 34.09 h for the 9th passage $p75^+$ EMSCs, a difference that showed no statistical significance ($p > 0.05$). In the MTT assay, a slightly higher OD value was detected for the 3rd passage $p75^+$ EMSCs at days 5 and 7 (Fig. 2B), although significant differences were not found ($p > 0.05$). Cell-cycle assays showed a similar percentage of cells shifting to the S phase (Fig. 2C and D). The results indicated that the proliferative activity of $p75^+$ EMSCs was stable *in vitro* during cell passaging.

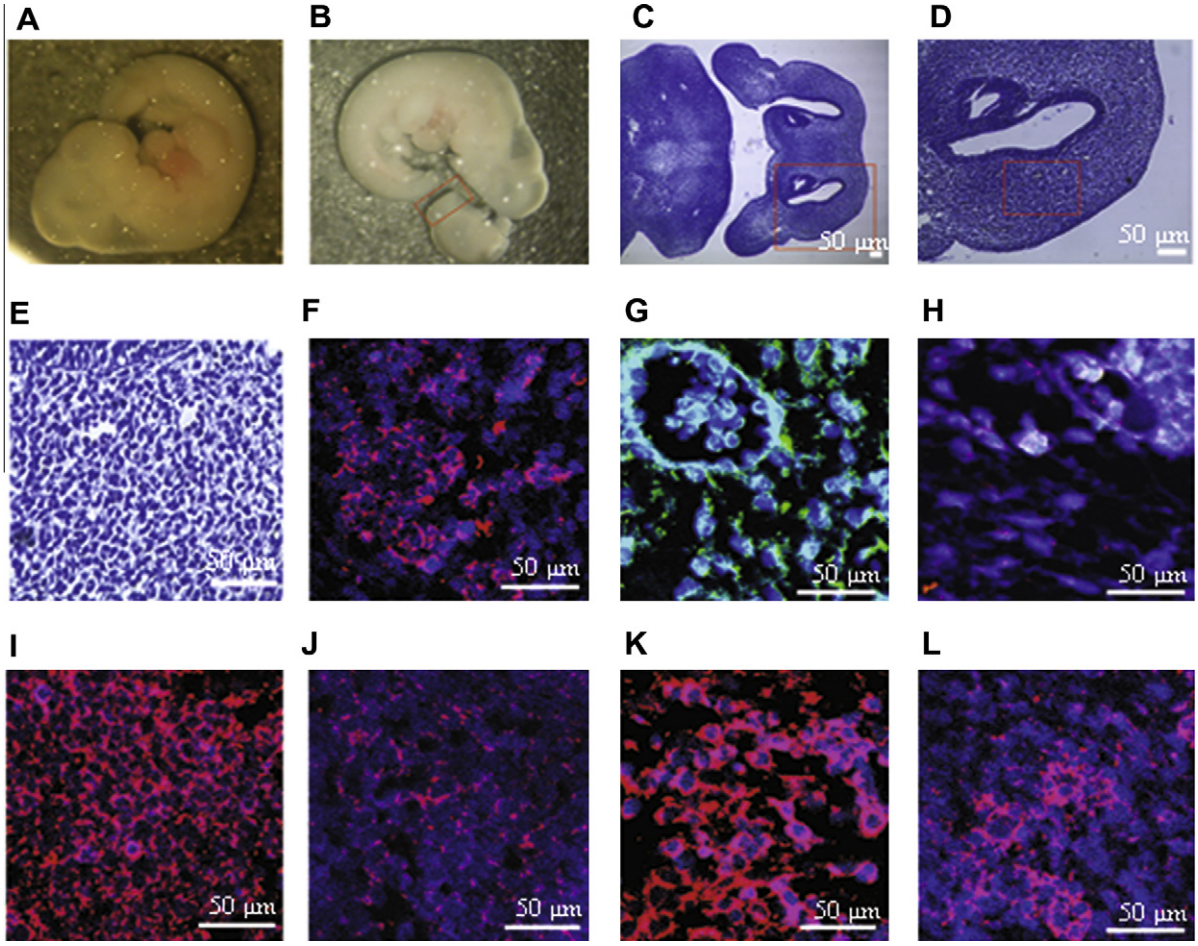

Fig. 1. Immunohistochemical staining of SD rat embryo facial process tissues. (A) Embryo from an E11.5 SD rat. (B) Embryo facial processes were dissected. (C–E) H.E. staining of rat embryo facial process at different levels of magnification. Embryonic facial processes comprised mostly of mesenchymal tissue containing large numbers of cells, whereas epithelial invagination or tooth-like epithelium was not observed. (F–L) Immunofluorescence staining of rat embryo facial process. Cells positive for P75NTR (F), Stro-1 (G), both P75NTR and Stro-1 (H), CD29 (I), CD44 (J), CD90 (K), and CD105 (L) present in rat embryo facial processes (scale bar, 50 μm).

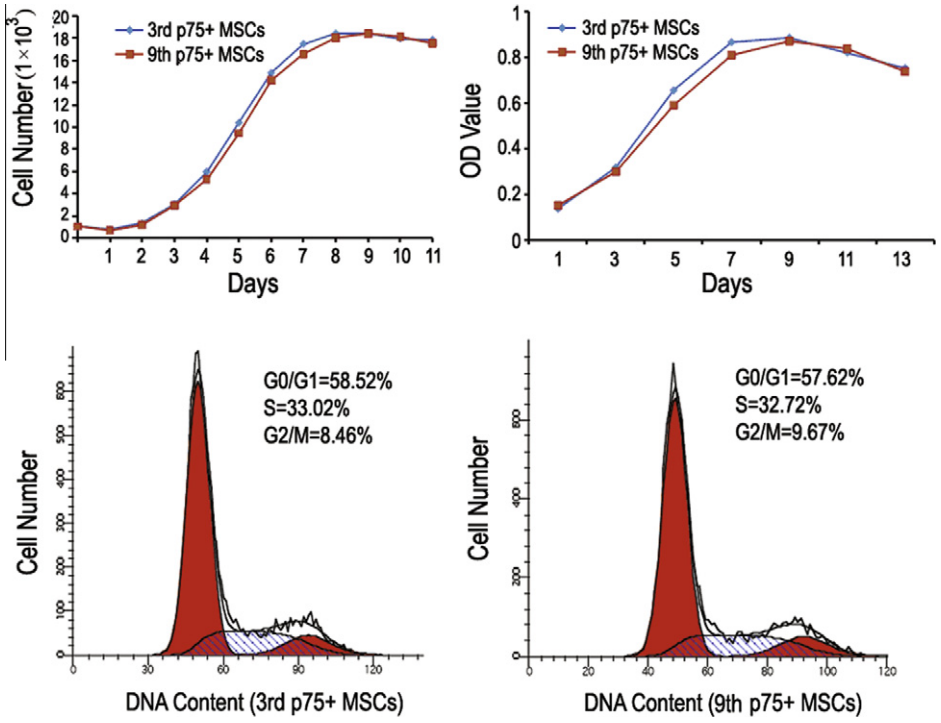

Fig. 2. Growth curves and proliferative activities of the p75$^+$ EMSCs at different passages. (A) 3rd and 9th passage p75$^+$ EMSCs both began to grow exponentially at day 2, reaching their peaks on days 8 and 9, respectively. No significant difference was found between them. (B) In the MTT assay, higher OD values were seen for the 3rd passage p75$^+$ EMSCs on days 5 and 7 than for the 9th passage p75$^+$ EMSCs, although these differences were not significant. (C and D) The cell-cycle assay results indicated that similar percentages of 3rd passage p75$^+$ EMSCs (33.02%) and 9th passage p75$^+$ EMSCs (32.72%) shifted to the S phase.

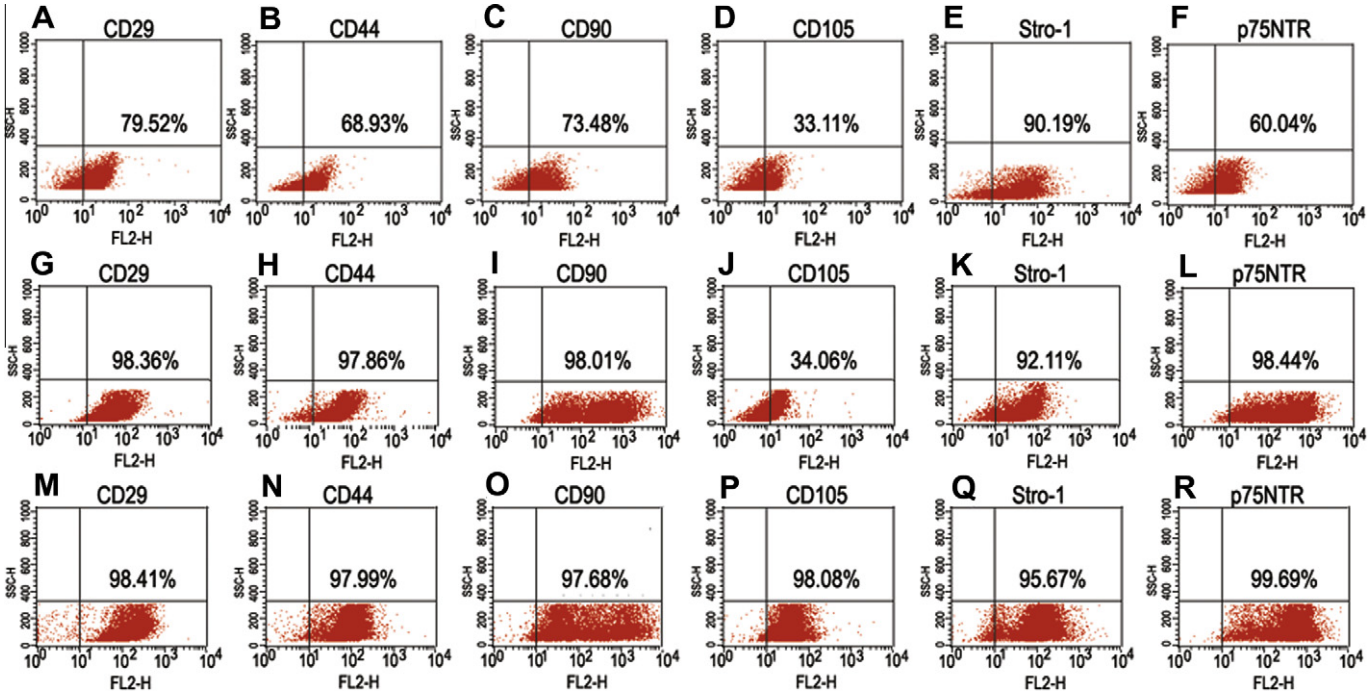

Fig. 3. Flow cytometric analysis of the expression levels of the following cell surface markers: CD29, CD44, CD90, CD105, Stro-1 and p75NTR in EMSCs (A–F), as well as 3rd (G–L) and 9th (M–R) passage p75$^+$ EMSCs.

Cell phenotype analysis using flow cytometry showed that p75NTR-positive cells of the 3rd and 9th passage p75$^+$ EMSCs accounted for 98.44% (Fig. 3L) and 99.69% (Fig. 3R) of the cells present, which was significantly higher than that for EMSCs before selection (60.04%) (Fig. 3F). This finding indicated that p75$^+$ EMSCs had been purified and showed little change in p75NTR expression during cell passaging. Similar results were found for the expression of CD29, CD44 and CD90 (Fig. 2A–C, G–I, M–O). Stro-1 was highly expressed in all three cell populations (Fig. 2E, K and Q), which indicated that most cells from the embryonic facial process were mesenchymal stem cells. An exception was CD105, which was highly expressed in the 9th passage p75$^+$ EMSCs (Fig. 2P) while being expressed at

relatively low levels in both 3rd passage p75$^+$ EMSCs and EMSCs (Fig. 2D and J). This result may imply a possibly higher proliferative activity for the 9th passage p75$^+$ EMSCs because CD105 has been reported to be associated with proliferation [17].

3.4. Multipotential differentiation ability of p75$^+$ EMSCs

p75$^+$ EMSCs in chemically defined conditions were induced to differentiate into mature adipocytes, osteocytes, chondrocytes or neuronal cells. In adipogenic medium, p75$^+$ EMSCs underwent a morphologic change from being fibroblast-like to elliptical, while the cell body also increased in size. Lipid droplets visualized with Oil Red-O staining appeared to have accumulated in the cytoplasm (Fig. 4A). The adipogenic differentiation of p75$^+$ EMSCs was further confirmed by the RT-PCR results that indicated the strong expression levels of *LPL* and *PPARγ2 mRNA* (Fig. 4B).

In an osteogenic medium, p75$^+$ EMSCs changed from a fibroblast-like state to a multilateral form after 4 days, developing a cuboidal shape and displaying a tightly packed arrangement at two weeks. Abundant mineralized nodules showing Alizarin red staining (Fig. 4C) and strong expression levels of *OCN* and *Col I mRNA* (Fig. 4D) were detected among the treated p75$^+$ EMSCs, although they were not observed among the untreated p75$^+$ EMSCs, except for the slight expression of *Col I mRNA*.

In a chondrogenic medium, p75$^+$ EMSCs were enlarged while becoming flat and polygonal in shape. A large amount of cartilage matrix was formed that showed positive Alcian blue staining (Fig. 4E). Strong expression levels of *AGG* and *Col II mRNA* were detected among the treated p75$^+$ EMSCs, while no or little expression was observed in untreated p75$^+$ EMSCs (Fig. 4F).

In a neurogenic medium, some of the p75$^+$ EMSCs underwent neuron-like morphologic changes: the cells' processes became thinner and longer, and the cytoplasm around the nucleus shrunk. The treated p75$^+$ EMSCs were NF-M positive, as observed using confocal laser scanning microscopy (Fig. 4G). The expression of *NF-M* and *MAP-2* was detected among the treated p75$^+$ EMSCs (Fig. 4H), but not among the untreated p75$^+$ EMSCs.

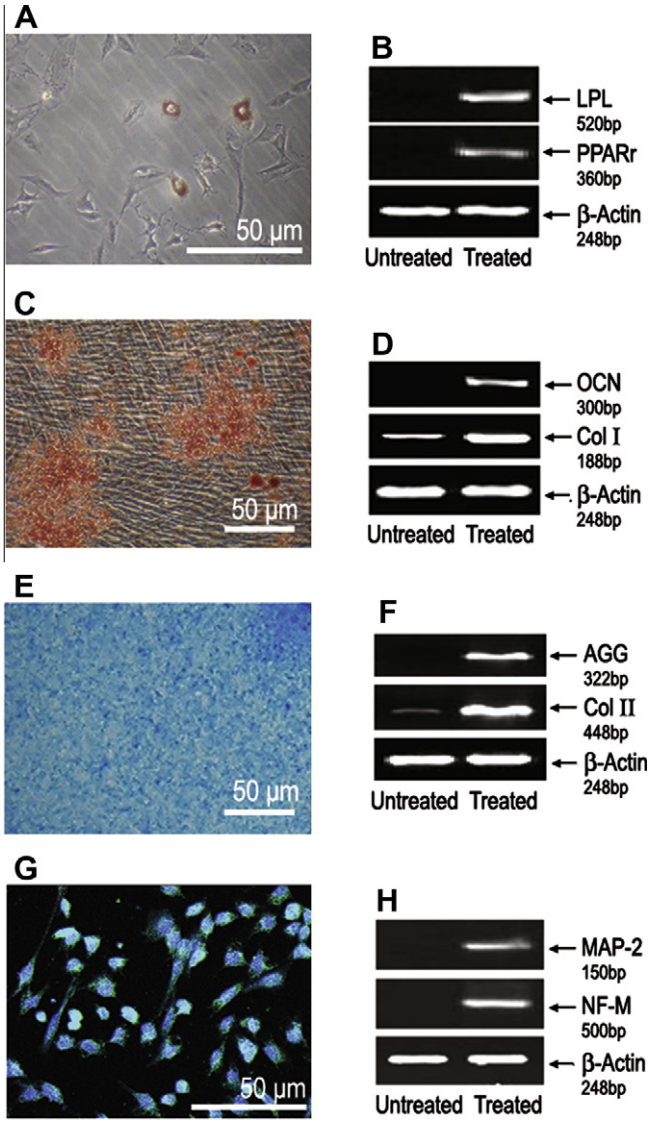

Fig. 4. Multipotent differentiation of p75$^+$ EMSCs. (A and B) Adipogenic induction. Treated p75$^+$ EMSCs formed lipid droplets as visualized with Oil Red-O staining and showed strong expression of specific genes (*LPL PPARγ2* mRNA), which were not detected among the untreated p75$^+$ EMSCs. (C and D) Osteogenic induction. An abundance of mineralized nodules was observed among the treated p75$^+$ EMSCs using Alizarin red staining, while the mineralization-related markers of *OCN*, *Col I* mRNA were strongly expressed. The slight expression of *Col I* mRNA was detected among the untreated p75$^+$ EMSCs. (E and F) Chondrogenic induction. Cartilage matrix with Alcian blue staining and the strong expression of *AGG* and *Col II* mRNA, which were not expressed or expressed only at low levels among the untreated p75$^+$ EMSCs, were observed among the treated p75$^+$ EMSCs. (G and H) Neuron-like induction. Confocal laser scanning microscopy and RT-PCR assays showed strong expression levels of NF-M and MAP-2 among the treated p75$^+$ EMSCs, whereas no expression was detected among the untreated p75$^+$ EMSCs (scale bar, 50 μm).

4. Discussion

Stem cells, defined as those cells possessing an intrinsic self-renewal ability and multilineage potential, have greatly contributed to the field of regenerative medicine. To understand the potential characteristics of stem cells harvested from immature tissues, the following three issues are important: (1) identification of the present stage of development of these cells, (2) purification of these cells, and (3) determination of stable proliferative behavior and multipotency.

In mice, tooth initiation is triggered by the reciprocal interaction between the dental epithelium and ectomesenchyme, which is derived from the neural crest and the first mandibular arch mesenchyme, via extracellular signaling factors at approximately E10 [18]. The data in this study indicated that EMSCs had migrated to the embryonic facial process at E11.5 in rats, while epithelial mesenchymal interactions were likely limited at this stage as epithelial invagination or tooth-like epithelium was not observed. Slight differences in the timing of these events between rats and mice reflect the shorter gestation period in mice [18,19]. This result is important both to our understanding of the fate of EMSCs at this site and to identifying the stage of development at which stem cells might be usefully exploited in tissue-engineering applications.

As reported by others, cell cultures harvested via enzymatic dissociation can give rise to heterogeneous cell populations [20]; this heterogeneity was significantly reduced after cell selection in the present study. Moreover, selected p75$^+$ EMSCs showed relatively stable proliferative activity and phenotypes during cell expansion to the 9th passage, on the basis of the growth curve and cell cycle analyses and MTT assay and flow cytometry results. Previous studies have reported that neural crest cells *in vitro* have a tendency to spontaneously differentiate along smooth muscle cells or osteoblast lineages in the absence of LIF, an inhibitor of differentiation of mouse embryonic stem cells [8,21,22]. In the present study, p75$^+$ EMSCs up to nine passages showed a relatively stable proliferative activity and the expression of the stem cell surface markers STRO-1, CD29, CD44, and CD90, as well as an increased expression of CD105, a component of the transforming growth factor-beta

receptor (TGF-betaR) complex associated with proliferation [17]. The data indicated that p75$^+$ EMSCs maintained an active renewal potential and showed no evidence of spontaneous differentiation during cell passage. A possible reason for these differences in the behavior of these cells is that the cells excluded by FACS, as well as their products, may play crucial roles in the spontaneous differentiation of neural crest cells, thereby reinforcing the view that the fate of pluripotent neural crest cells may be determined by their environment [23].

Stro-1, a widely accepted marker for mesenchymal stem cells, has been used to select adult stem cells in many studies [24,25]. In previous studies, Stro-1-expressing cells accounted for approximately 20–40% of dental stem cells [20,26]. However, the present study showed a very high expression level of Stro-1 (i.e., more than 90%) both among p75$^+$ EMSCs cells and in the cells before selection. The data indicated that the proportion of stem cells in cultures from embryonic tissue was much larger than that from mature tissues, suggesting a potential application of embryonic tissue-derived stem cells in the engineering of tissues and organ systems. In contrast with Stro-1, in this study, p75NTR was differentially expressed between the p75$^+$ EMSCs (more than 99%) and the cells prior to selection (60.04%), indicating that Stro-1-positive cells might include cells with an origin other than the neural crest. Therefore, we propose that p75NTR, rather than Stro-1, be considered an optimal marker for the selection of dental stem cells of neural crest origin.

The multipotency of neural crest cells is suggested by their capacity to give rise to odontoblasts, pulp cells, osteoblasts, and chondrocytes, which all form the orofacial tissues during development [27,28]. However, only limited information regarding cell lineage diversity is available from *in vitro* experiments. In the current study, the formation of lipid droplets, mineralized nodules, and the cartilage extracellular matrix, as well as the detection of NF-M immunofluorescent-positive cells in the p75$^+$ EMSCs after treatment with various chemically defined conditions, demonstrated the adipogenic, osteogenic, chondrogenic and neurogenic differentiation potential of these cells. The RT-PCR results further confirmed the *in vitro* multilineage potential of p75$^+$ EMSCs, which suggested their potential application in tissue engineering and regenerative strategies for teeth.

In conclusion, in this study, we confirmed the presence of p75NTR positive cells in embryonic facial processes of E11.5 SD rats and the non-appearance of an epithelial invagination or tooth-like epithelium. p75$^+$ EMSCs isolated from rat embryonic facial processes showed a stable proliferation pattern, phenotype and multipotential differentiation capacity *in vitro*. This characterization of p75$^+$ EMSCs in this study led to favorable results and highlighted its advantages in the cell aggregate technique that mimicks cell-to-cell and epithelial–mesenchymal interactions in the bioengineered tooth germ [29]. Moreover, p75$^+$ EMSCs may provide an *in vitro* model that contributes to our understanding of those mechanisms underlying epithelial–mesenchymal interactions in tooth morphogenesis. Further studies are necessary to investigate both the *in vitro* and *in vivo* biological properties of these cells as well as their potential for use in odontogenesis.

Acknowledgments

This work was supported by grants from the National Natural Science Foundation of China (Grant No. 31070863) and from the Natural Science Foundation Project of Chongqing, China (Grant Nos. CSTC2010BB5161 and CSTC2011BA5013).

Appendix A. Supplementary data

Supplementary data associated with this article can be found, in the online version, at http://dx.doi.org/10.1016/j.bbrc.2012.08.109.

References

[1] L. Casagrande, M.M. Cordeiro, S.A. Nör, J.E. Nör, Dental pulp stem cells in regenerative dentistry, Odontology 99 (2011) 1–7.
[2] V. Yu, M. Damek-Poprawa, S.B. Nicoll, S.O. Akintoye, Dynamic hydrostatic pressure promotes differentiation of human dental pulp stem cells, Biochem. Biophys. Res. Commun. 386 (2009) 661–665.
[3] C. Martínez, P.C. Smith, J.P. Rodriguez, V. Palma, Sonic hedgehog stimulates proliferation of human periodontal ligament stem cells, J. Dent. Res. 90 (2011) 483–488.
[4] A. Balic, M. Mina, Characterization of progenitor cells in pulps of murine incisors, J. Dent. Res. 89 (2010) 1287–1292.
[5] A.S. Tucker, P.T. Sharpe, Molecular genetics of tooth morphogenesis and patterning: the right shape in the right place, J. Dent. Res. 78 (1999) 826–834.
[6] Y. Chai, X. Jiang, Y. Ito, P.Jr. Bringas, J. Han, D. Rowitch, P. Soriano, A.P. McMahon, H.M. Sucov, Fate of the mammalian cranial neural crest during tooth and mandibular morphogenesis, Development 127 (2000) 1671–1679.
[7] H. Kapadia, G. Mues, R. D'Souza, Genes affecting tooth morphogenesis, Orthod. Craniofac. Res. 10 (2007) 237–244.
[8] M.J. Deng, Y. Jin, J.N. Shi, H.B. Lu, Y. Liu, D.W. He, X. Nie, A.J. Smith, Multilineage differentiation of ectomesenchymal cells isolated from the first branchial arch, Tissue Eng. 10 (2004) 1597–1606.
[9] X. Nie, Y.J. Zhang, W.D. Tian, M. Jiang, D. Rui, J.W. Chen, Y. Jin, Improvement of peripheral nerve regeneration by a tissue–engineered nerve filled with ectomesenchymal stem, Int. J. Oral Maxillofac. Surg. 36 (2007) 32–38.
[10] S.J. Morrison, P.M. White, C. Zock, D.J. Anderson, Prospective identification isolation by flow cytometry and in vivo self-renewal of multipotent mammalian neural crest stem cells, Cell 96 (1999) 737–749.
[11] I. Moscatelli, E. Pierantozzi, A. Camaioni, G. Siracusa, L. Campagnolo, p75 neurotrophin receptor is involved in proliferation of undifferentiated mouse embryonic stem cells, Exp. Cell Res. 315 (2009) 3220–3232.
[12] J. Zhang, X. Duan, H. Zhang, Z. Deng, Z. Zhou, N. Wen, A.J. Smith, W. Zhao, Y. Jin, Isolation of neural crest-derived stem cells from rat embryonic mandibular processes, Biol. Cell 98 (2006) 567–575.
[13] N. Yamamoto, H. Akamatsu, S. Hasegawa, T. Yamada, S. Nakata, M. Ohkuma, E. Miyachi, T. Marunouchi, K. Matsunaga, Isolation of multipotent stem cells from mouse adipose tissue, J. Dermatol. Sci. 48 (2007) 43–52.
[14] D. Woodbury, E.J. Schwarz, D.J. Prockop, I.B. Black, Adult rat and human bone marrow stromal cells differentiate into neurons, J. Neurosci. Res. 61 (2000) 364–370.
[15] X. Wen, X. Nie, L. Zhang, L. Liu, M. Deng, Adipose tissue-deprived stem cells acquire cementoblast features treated with dental follicle cell conditioned medium containing dentin non-collagenous proteins in vitro, Biochem. Biophys. Res. Commun. 409 (2011) 83–589.
[16] Y. Li, J. Li, S. Zhu, E. Luo, G. Feng, Q. Chen, J. Hu, Effects of strontium on proliferation and differentiation of rat bone marrow mesenchymal stem cells, Biochem. Biophys. Res. Commun. 418 (2012) 725–730.
[17] J. Qi, A. Chen, H. You, K. Li, D. Zhang, F. Guo, Proliferation and chondrogenic differentiation of CD105-positive enriched rat synovium-derived mesenchymal stem cells in three-dimensional porous scaffolds, Biomed. Mater. 6 (2011) 015006.
[18] D.S. Koussoulakou, L.H. Margaritis, S.L. Koussoulakos, A curriculum vitae of teeth: evolution generation regeneration, Int. J. Biol. Sci. 5 (2009) 226–243.
[19] J.J. Bustamante, G. Dai, M.J. Soares, Pregnancy and lactation modulate maternal splenic growth and development of the erythroid lineage in the rat and mouse, Reprod. Fertil. Dev. 20 (2008) 303–310.
[20] A. Bakopoulou, G. Leyhausen, J. Volk, A. Tsiftsoglou, P. Garefis, P. Koidis, W. Geurtsen, Comparative analysis of in vitro osteo/odontogenic differentiation potential of human dental pulp stem cells (DPSCs) and stem cells from the apical papilla (SCAP), Arch. Oral Biol. 56 (2011) 709–721.
[21] S.J. Morrison, N.M. Shah, D.J. Anderson, Regulatory mechanisms in stem cell biology, Cell 88 (1997) 287–298.
[22] L.S. Wright, J. Li, M.A. Caldwell, K. Wallace, J.A. Johnson, C.N. Svendsen, Gene expression in human neural stem cells: effects of leukemia inhibitory factor, J. Neurochem. 86 (2003) 179–195.
[23] P.H. Patterson, Control of cell fate in a vertebrate neurogenic lineage, Cell 62 (1990) 1035–1038.
[24] J. Xu, W. Wang, Y. Kapila, J. Lotz, S. Kapila, Multiple differentiation capacity of STRO-1+/CD146+ PDL mesenchymal progenitor cells, Stem Cells Dev. 18 (2009) 487–496.
[25] X. Yang, J. van den Dolder, X.F. Walboomers, W. Zhang, Z. Bian, M. Fan, J.A. Jansen, The odontogenic potential of STRO-1 sorted rat dental pulp stem cells in vitro, J. Tissue Eng. Regen. Med. 1 (2007) 66–73.
[26] E.T. Guimarães, G.S. Cruz, A.A. de Jesus, A.F. Lacerda de Carvalho, S.R. Rogatto, V. Pereira Lda, R. Ribeiro-dos-Santos, M.B. Soares, Mesenchymal and embryonic characteristics of stem cells obtained from mouse dental pulp, Arch. Oral Biol. 56 (2011) 1247–1255.
[27] R.M. Langille, M. Solursh, Formation of chondrous and osseous tissues in micromass cultures of rat frontonasal and mandibular ectomesenchyme, Differentiation 44 (1990) 197–206.
[28] N.M. Le Douarin, S. Creuzet, Neural crest and vertebrate evolution, Biol. Aujourdhui. 205 (2011) 87–94.
[29] S. Gronthos, D.M. Franklin, H.A. Leddy, P.G. Robey, R.W. Storms, J.M. Gimble, Surface protein characterization of human adipose tissue-derived stromal cells, J. Cell. Physiol. 189 (2001) 54–63.